Nonlinear Modeling of the Dynamic Effects of Infused Insulin on Glucose: Comparison of Compartmental With Volterra Models

Nonlinear Modeling of the Dynamic Effects of Infused Insulin on Glucose: Comparison of Compartmental With Volterra Models

Georgios D. Mitsis*, *Member, IEEE*, Mihalis G. Markakis, *Student Member, IEEE*, and Vasilis Z. Marmarelis, *Fellow, IEEE*

***Abstract*—This paper presents the results of a computational study that compares simulated compartmental (differential equation) and Volterra models of the dynamic effects of insulin on blood glucose concentration in humans. In the first approach, we employ the widely accepted "minimal model" and an augmented form of it, which incorporates the effect of insulin secretion by the pancreas, in order to represent the actual closed-loop operating conditions of the system, and in the second modeling approach, we employ the general class of Volterra-type models that are estimated from input–output data. We demonstrate both the equivalence between the two approaches analytically and the feasibility of obtaining accurate Volterra models from insulin–glucose data generated from the compartmental models. The results corroborate the proposition that it may be preferable to obtain data-driven (i.e., inductive) models in a more general and realistic operating context, without resorting to the restrictive prior assumptions and simplifications regarding model structure and/or experimental protocols (e.g., glucose tolerance tests) that are necessary for the compartmental models proposed previously. These prior assumptions may lead to results that are improperly constrained or biased by preconceived (and possibly erroneous) notions—a risk that is avoided when we let the data guide the inductive selection of the appropriate model within the general class of Volterra-type models, as our simulation results suggest.**

***Index Terms*—Laguerre–Volterra networks (LVNs), physiological systems, Volterra–Wiener models.**

I. Introduction

DIABETES mellitus represents an alarming threat to public health with rising trends and severity in recent years worldwide, and is characterized by multiple and often not readily observable clinical effects [1]. There is, therefore, urgent need for improved diagnostic methods that provide more precise clinical assessments and sensitive detection of symptoms at earlier stages of the disease. This critical task may be facilitated (or enabled) by the utilization of advanced mathematical models that reliably describe the dynamic interrelationships among key physiological variables implicated in the underlying physiology (i.e., blood glucose concentration and various hormones such as insulin, glucagon, epinephrine, norepinephrine, cortisol, etc.) under a variety of metabolic and behavioral conditions (e.g., pre-/postprandial, exercise/rest, and stress/relaxation). Such models would not only provide a powerful diagnostic tool, but may also enable long-term glucose regulation in diabetics through closed-loop model-reference control using frequent insulin microinfusions administered by implanted programmable micropumps. This will prevent the onset of the pathologies caused by elevated blood glucose over prolonged periods in diabetic patients [1].

Blood glucose concentration fluctuates considerably in response to food intake, hormonal cycles, or behavioral factors. These fluctuations may range from 70 to 180 mg/dL in most normal subjects, although blood glucose concentration remains within the normoglycemic zone (70–110 mg/dL [2]) for most of the time. The internal physiological regulation of these wide fluctuations is a complex, multifactorial process. The most critical regulatory role is played by the pancreas, which, upon sensing an elevation in blood glucose concentration, secretes insulin through its beta cells, while an opposite change in glucose causes secretion of glucagon through its alpha cells. The secreted insulin assists the uptake of glucose by the cells and the storage of excess glucose in the liver in the form of glycogen. Secreted glucagon assists the catabolism of glycogen into glucose that is released from the liver into the bloodstream, while insulin inhibits glycogen synthase [3]. Furthermore, free fatty acids in the blood potentiate the short-term responsiveness of pancreatic beta cells to glucose oscillations, but may inhibit long-term responsiveness [4], [5]. Finally, blood glucose concentration and its relation to insulin concentration depend on the action of several other hormones (e.g., epinephrine, norepinephrine, and cortisol [6]–[8]), making the daunting complexity of this multifactorial regulatory mechanism evident.

The primary effect on blood glucose is exercised by insulin, and most efforts to date have focused on the study of this causal relationship. Prolonged hyperglycemia is usually caused by defects in insulin secretion by the pancreatic beta cells or in the efficiency of insulin-facilitated glucose uptake by the cells.

Manuscript received August 1, 2008; revised December 2, 2008 and March 25, 2009. First published June 2, 2009; current version published September 16, 2009. This work was supported in part by the European Social Fund and National Resources—Operational Program Competitiveness—General Secretariat for Research and Development (Program ENTER), in part by the National Institute of Health (NIH)/the National Institute of Biomedical Imaging and Bioengineering (NIBIB) Center under Grant P41-EB001978 to the Biomedical Simulations Resource, University of Southern California, and in part by Myronis Foundation (Graduate Research Scholarship). *Asterisk indicates corresponding author.*

*G. D. Mitsis was with the Institute of Communications and Computer Systems, National Technical University of Athens, Athens 15780, Greece. He is now with the Department of Electrical and Computer Engineering, University of Cyprus, Nicosia 1678, Cyprus (e-mail: gmitsis@ucy.ac.cy).

M. G. Markakis is with the Department of Electrical Engineering and Computer Science, Massachusetts Institute of Technology, Cambridge, MA 02139 USA (e-mail: mihalis@mit.edu).

V. Z. Marmarelis is with the Department of Biomedical Engineering, University of Southern California, Los Angeles, CA 90089 USA (e-mail: vzm@bmsr.usc.edu).

Digital Object Identifier 10.1109/TBME.2009.2024209

The exact quantitative nature of the dependence between blood glucose concentration and the action of the other hormones mentioned before, or factors such as diet, endocrine cycles, exercise, stress, etc., remains largely unknown (primarily because of lack of appropriate data), although the qualitative effect has been established. Thus, the aggregate effect of all these other factors for modeling purposes is viewed as random "disturbances," additive to the blood glucose level.

Starting from the initial work of Bolie [9] and Ackerman *et al.* [10], most modeling studies of the causal relationship between insulin and glucose (as the "input" and "output" of a system representing this relationship) have relied on the concept of compartmental modeling [11]. In this context, the minimal model (MM) of glucose disappearance, combined with the intravenous glucose tolerance test (IVGTT), has been the most widely used method to study whole body glucose metabolism *in vivo* [12], [13]. The MM postulates that insulin acts from a remote compartment and affects glucose utilization, in addition to the insulin-independent utilization that depends on the glucose level *per se*. These insulin-dependent and insulin-independent effects on glucose utilization/kinetics are combined in a single compartment. Certain parameters of the MM (i.e., insulin resistance S_I and glucose sensitivity S_G) have been shown to be of clinical importance, and can be estimated from IVGTT data, using nonlinear least-squares methods [14], [15] or, more recently, Bayesian estimation techniques [16]–[18].

However, the accuracy of the estimates obtained from the MM has been questioned because of the single-compartment assumption [15], [19], [20], and two-compartment models for glucose kinetics [21]–[23], as well as multicompartmental models for glucose and insulin kinetics, have been proposed [24], [25]. Other modeling approaches that have been recently explored—in the context of glucose control—include artificial neural networks [26], probabilistic models [27], and linear/nonlinear impulse response and Volterra models [28], [29]. In addition to these insulin–glucose models, attempts have been made to take into account the influence of some relevant physiological signals, such as glucagon [24], [25] and free fatty acids [30].

The aforementioned compartmental models rely on *a priori* assumptions and simplifications regarding the underlying physiological mechanisms, and their primary aim is often to extract clinically important parameters in conjunction with specific experimental protocols (e.g., the IVGTT). Therefore, their ability to quantify glucose metabolism under actual, more general operating conditions remains limited. On the other hand, recent technological advances in the development of reliable continuous glucose sensors and insulin micropumps [31], [32] have provided time-series data that enable the application of data-true modeling approaches [33]. These approaches offer new opportunities toward the goal of obtaining reliable models of the insulin–glucose interrelationships in a more general context. Using spontaneous or externally infused insulin and glucose data, one can obtain data-driven models that are not constrained by *a priori* assumptions regarding their structure.

The present paper examines the relation between existing compartmental (differential equation) and Volterra-type models, both analytically and computationally. The results demonstrate the feasibility of obtaining Volterra models of insulin–glucose dynamics that are equivalent to widely accepted compartmental models, using data records that are practically obtainable. They also illustrate the physiological interpretation of nonlinear Volterra models by providing direct links to a well-known parametric model with parameters of clinical significance. Since the Volterra approach does not require prior assumptions about model structure, it can provide the effective means for obtaining accurate data-true, patient-specific, and time-adaptive models in a clinical context.

II. Methods

The present study concerns compartmental and Volterra-type nonlinear dynamic models; among compartmental models, we select the MM of glucose disappearance, as well as an augmented version of it [augmented MM (AMM)], which incorporates an insulin secretion equation. The structure and parameter values of these models are taken from the literature [12], [14], [34]–[37]. The equivalent Volterra models [38] are estimated using simulated input–output data from the compartmental models.

A. MM of Glucose Disappearance

The MM of glucose disappearance is described by the following two differential equations [12], which describe the nonlinear dynamics of the insulin-to-glucose relationship during an IVGTT:

$$\frac{dg(t)}{dt} = -p_1 g(t) - x(t)[g(t) + g_b] \tag{1}$$

$$\frac{dx(t)}{dt} = -p_2 x(t) + p_3 i(t) \tag{2}$$

where $g(t)$ is the deviation of glucose plasma concentration from its basal value g_b (in milligrams per deciliter), $x(t)$ is the "internal variable" of insulin action (in minutes inverse), $i(t)$ is the deviation of insulin plasma concentration from its basal value i_b (in microunits per milliliter), p_1 and p_2 are the parameters describing the kinetics of glucose and insulin action, respectively (in minutes inverse), and p_3 is a parameter (in inverse of minutes square·milliliters per microunit) that affects insulin sensitivity (see next). The initial conditions for the simulations are: $g(0) = 0$ and $x(0) = 0$ (i.e., we assume that we start at basal conditions, which is a reasonable assumption in the context of simulating the model for situations where the initial "transient" phase can be ignored). Note that the MM is nonlinear, due to the presence of the bilinear term between the internal variable $x(t)$ representing insulin action and the variable $[g(t) + g_b]$ representing the plasma glucose concentration in the first equation. This bilinear term describes the modulation of the effective kinetic constant of the glucose utilization by insulin action (i.e., increases in insulin concentration cause faster disappearance of blood glucose).

The physiological interpretation of the MM parameters can be made in terms of insulin-dependent and insulin-independent processes that enhance glucose uptake and suppress net glucose output [13]. The parameter p_1, termed "glucose effectiveness"

S_G, represents the insulin-independent effect, while the insulin-dependent effect is represented by the ratio p_3/p_2 [in inverse of minutes square per (microunit·inverse of milliliter)], and is termed "insulin sensitivity" S_I. The values of S_G and S_I are typically estimated from IVGTT data, and the MM has proven to be successful in a clinical context, requiring a relatively simple test procedure [13]. Nonetheless, the accuracy and physiological interpretation of the MM parameter estimates have been questioned because of the use of a single compartment for glucose kinetics [19], [20].

The MM, as formulated in (1) and (2), does not include an equation describing the secretion of insulin from pancreatic beta cells in response to an elevation in blood glucose concentration, i.e., it is an open-loop model, which may be used along with properly designed experimental protocols (IVGTT) for parameter estimation. However, the actual glucose metabolism process is a closed-loop system, except in conditions of severe Type I diabetes where the pancreatic beta cells are considered totally inactive. In order to account for this, an insulin-secretion equation may be included, as described next (closed-loop MM or AMM). Limitations of the MM (and the AMM) include the absence of an explicit glucogenic component reflecting the production of new glucose by the liver in response to elevated plasma insulin, and/or glucose (such as the model presented in [39]) and the associated glucagon secretion process (from the alpha cells of the pancreas) among others. The aggregate effect of these processes, as well as the effect of other factors (free fatty acids, epinephrine, etc.), can be incorporated by "disturbance" terms that are added to the glucose rate and insulin action equations.

B. Closed-Loop Parametric Model: Augmented MM

The closed-loop nature of insulin–glucose interactions requires the incorporation of an additional equation describing the insulin secretion dynamics by the pancreatic beta cells. Of several equations that have been proposed [14], [36], [37], [40], [41], we select the one that utilizes a threshold function [see (5) and (6) next] [14], [36], [37]. The resulting closed-loop model becomes

$$\frac{dg(t)}{dt} + p_1 g(t) = -x(t)[g(t) + g_b] \tag{3}$$

$$\frac{dx(t)}{dt} = -p_2 x(t) + p_3[i(t) + r(t)] \tag{4}$$

$$\frac{dr(t)}{dt} = -ar(t) + \beta T_h[g(t)] \tag{5}$$

where $r(t)$ is the secreted insulin by the pancreatic beta cells in response to an elevation in plasma glucose concentration. The secretion is triggered by elevated plasma glucose concentrations according to the threshold function $T_h[g(t)]$ defined as

$$T_h[g(t)] = \begin{cases} g(t) - \theta, & g(t) \geq \theta \\ 0, & \text{otherwise} \end{cases} \tag{6}$$

where θ corresponds to the glucose concentration value above which insulin is secreted. The dynamics of this triggered secretion process and the kinetics of the secreted insulin are described (in first approximation) by the kinetic constant a (in minutes inverse) in (5). The parameter β [in microunits·inverse of minutes square per (milliliter·milligram per deciliter)] determines the rate of insulin secretion (i.e., the strength of the feedback pathway).

C. Volterra-Type Modeling

The Volterra–Wiener framework has been employed extensively for modeling nonlinear physiological systems [38]. In this context, the input–output dynamic relationship of a causal, nonlinear system of order Q and memory M is described by the Volterra functional expansion as

$$g(t) = \sum_{n=0}^{Q} \int_0^M \cdots \int_0^M k_n(\tau_1, \ldots, \tau_n) \times i(t-\tau_1) \ldots i(t-\tau_n) d\tau_1 \ldots d\tau_n \tag{7}$$

where $i(t)$ and $g(t)$ are the input and output of the system at time t (deviations of plasma insulin and glucose concentrations from their basal values, respectively). The unknown quantities of the Volterra model that are estimated from the input–output data are the Volterra kernels $k_n(\tau_1, \ldots, \tau_n)$. The first-order kernel ($n = 1$) is the linear component of the system dynamics, while the higher order kernels ($n > 1$) form a hierarchy of the nonlinear dynamics of the system. The highest order Q defines the nonlinear order of the system. Many physiological systems can be described adequately by Volterra models of second or third order [38]. The Volterra–Wiener approach is well suited to the complexity of physiological systems since it yields data-true models, without requiring *a priori* assumptions about system structure.

Among various methods that have been developed for the estimation of the discretized Volterra kernels, a Volterra-equivalent network in the form of the Laguerre–Volterra network (LVN) is selected because it has been proven to be an efficient approach that yields accurate representations of high-order systems in the presence of noise using short input–output records [42]. The LVN model consists an input layer of a Laguerre filter bank and a hidden layer of K hidden units with polynomial activation functions (see Fig. 1) [42]. At each discrete time t, the input signal $i(t)$ (insulin) is convolved with the Laguerre filter bank and weighted sums of the filter bank outputs v_j (where $v_j = i * b_j$, and b_j is the jth-order discrete-time Laguerre function) are transformed by the hidden units through polynomial transformations.

The model output $g(t)$ (glucose) is formed as the summation of the hidden unit outputs z_k and a constant corresponding to the glucose basal value g_b as

$$u_k(t) = \sum_{j=0}^{L-1} w_{k,j} v_j(t) \tag{8}$$

$$g(t) = \sum_{k=1}^{K} z_k(t) + g_b = \sum_{k=1}^{K} \sum_{n=1}^{Q} c_{n,k} u_k^n(t) + g_b \tag{9}$$

where L is the number of functions in the filter bank, and $w_{k,j}$ and $c_{q,k}$ are the weighting and polynomial coefficients,

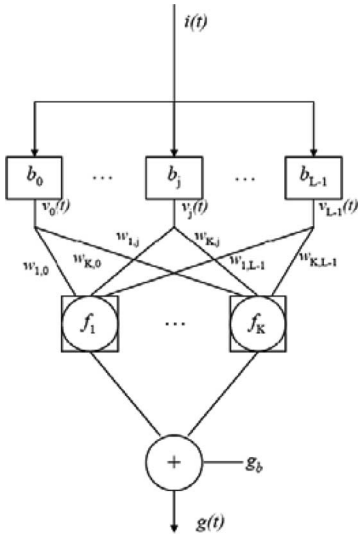

Fig. 1. LVN. The system input $i(t)$ is convolved with a Laguerre filter bank with impulse responses b_j, the outputs of which ($v_j(n)$) are fed into a layer of K hidden units with polynomial activation functions f_K that produce the system output $g(t)$.

respectively. The insulin and glucose time series are used to train the LVN model parameters ($w_{k,j}, c_{q,k}$, and the Laguerre parameter that determines the Laguerre functions dynamic properties) with a gradient-descent algorithm as follows [42]:

$$\delta^{(r+1)} = \delta^{(r)} + \gamma_\beta \varepsilon^{(r)}(n) \sum_{k=1}^{n} f_k'^{(r)}(u_k^{(r)}(n)) \times \sum_{j=0}^{L} w_{k,j}[v_j(n-1) + v_{j-1}(n)] \quad (10)$$

$$w_{k,j}^{(r+1)} = w_{k,j}^{(r)} + \gamma_w \varepsilon^{(r)}(n) f_k'^{(r)}(u_k^{(r)}(n)) v_j(n) \quad (11)$$

$$c_{m,k}^{(r+1)} = c_{m,k}^{(r)} + \gamma_c \varepsilon^{(r)}(n)(u_k^{(r)}(n))^m \quad (12)$$

where δ is the square root of the Laguerre parameter, γ_β, γ_w, and γ_c are the positive learning constants, r denotes iteration, and $\varepsilon^{(r)}(n)$ and $f_k'^{(r)}(u_k)$ are the output error and derivative of the polynomial activation function of the kth hidden unit, evaluated at the rth iteration, respectively.

The equivalent Volterra kernels are then obtained in terms of the LVN parameters as

$$k_n(\tau_1, \ldots, \tau_n) = \sum_{k=1}^{K} c_{n,k} \sum_{j_1=0}^{L-1} \cdots \sum_{j_n=0}^{L-1} w_{k,j_1} \ldots w_{k,j_n} b_{j_1}(\tau_1) \ldots b_{j_n}(\tau_n). \quad (13)$$

The structural parameters of the LVN model (L, K, and Q) are selected on the basis of the normalized mean-square error (NMSE) of the output prediction achieved by the model, defined as the sum of squares of the model residuals divided by the sum of squares of the demeaned true output. The statistical significance of the NMSE reduction achieved for model structures of increased order/complexity is assessed by comparing the percentage NMSE reduction with the *alpha*-percentile value of a chi-square distribution with p DOF (p is the increase of the number of free parameters in the more complex model) at a significance level *alpha*, typically set at 0.05 [44].

The LVN representation is equivalent to a variant of the general Wiener–Bose model termed the principal dynamic-mode (PDM) model. The PDM model consists of a set of parallel branches, each one of which is the cascade of a linear dynamic filter (PDM) followed by a static nonlinearity [38], [45]. Each of the K hidden units of the LVN corresponds to a separate branch, and defines the respective PDM $p_K(t)$ and polynomial nonlinearity. This leads to model representations that allow physiological interpretation, since the resulting number of branches is typically low in practice. According to the PDM model form, the insulin input signal is convolved with each of the PDMs $p_k(t)$, where $k = 1, \ldots, K$ and $p_k(t) = \sum_{j=0}^{L-1} w_{k,j} b_j(t)$, and the PDM outputs u_k are subsequently transformed by the respective polynomial nonlinearities $f_k(\cdot)$ to produce the model-predicted blood glucose output (the asterisk denotes convolution) as

$$g(t) = g_b + f_1[u_1(t)] + \cdots + f_K[u_K(t)] = g_b + f_1[p_1(t) * i(t)] + \cdots + f_K[p_K(t) * i(t)]. \quad (14)$$

D. Equivalence Between Compartmental and Volterra Models

In order to examine the mathematical relationship between the aforementioned compartmental and Volterra models, we employ the generalized harmonic balance method to derive analytical relations between the two model forms, as outlined next for the second-order case of the nonparametric model [46]. This procedure can be extended to any order of interest.

By setting the input $i(t)$ equal to 0, e^{st} and $e^{s_1 t} + e^{s_2 t}$ in the general Volterra model of (7) successively, the output $g(t)$ becomes equal to k_0, $k_0 + e^{st}K_1(s) + e^{2st}K_2(s,s) + \cdots$ and $k_0 + e^{s_1 t}K_1(s_1) + e^{s_2 t}K_1(s_2) + e^{(s_1+s_2)t}K_2(s_1, s_2) + \cdots$, where $K_1(s)$ and $K_2(s_1, s_2)$ are the Laplace transforms of $k_1(\tau)$ and $k_2(\tau_1, \tau_2)$, respectively. If we substitute these three input–output pairs into the differential equations of the compartmental models [(1) and (2) for the open-loop model, and (3) and (5) for the closed-loop model] and equate the coefficients of the resulting exponentials of the same kind, we can obtain analytical expressions for $k_0, K_1(s)$, and $K_2(s_1, s_2)$, in terms of the parameters of the respective compartmental model.

To define the computational equivalence between the two model forms, we simulate the compartmental models with broadband input (insulin) data, and we then estimate the kernels of the equivalent Volterra model from the simulated input–output data. The accuracy of the estimated first- and second-order Volterra kernels is assessed by comparison with the exact kernels of the equivalent Volterra model that are derived in analytical form from the differential equations of the compartmental models. The accuracy and robustness of the kernel estimates are evaluated under measurement noise conditions, in order to assess the performance of the Volterra approach.

III. Results

A. Analytical Expressions of the Volterra Kernels of the Compartmental Model: Open-Loop Case

The bilinear term between insulin action and glucose concentration in (1) of the MM gives rise to an equivalent Volterra model of infinite order. However, for parameter values within the physiological range, a second-order Volterra model offers an adequate approximation for all practical purposes. Considering the insulin and glucose deviations from the respective basal values $i(t)$ and $g(t)$ as the input and the output, respectively, we can derive analytically the Volterra kernels of the open-loop MM by applying the procedure outlined in Section II to the integro-differential equation

$$\dot{g}(t) + p_1 g(t) + p_3 \int_0^\infty \exp(-p_2\tau) i(t-\tau) g(t) d\tau = -g_b p_3 \int_0^\infty \exp(-p_2\tau) i(t-\tau) d\tau. \quad (15)$$

The aforementioned equation is derived from the MM by substituting the convolutional solution of (2)

$$x(t) = p_3 \int_0^\infty \exp(-p_2\tau) i(t-\tau) d\tau \quad (16)$$

into (1). Upon application of this method, we derive the following analytical expressions in the Laplace domain for the first- and second-order Volterra kernels of the MM ($k_0 = 0$):

$$K_1(s) = -p_3 g_b \frac{1}{(s+p_1)(s+p_2)} \quad (17)$$

$$K_2(s_1, s_2) = \frac{g_b p_3^2}{2} \frac{1}{(s_1+p_1)(s_1+p_2)} \times \frac{1}{(s_2+p_1)(s_2+p_2)} \left[1 + \frac{p_2}{s_1+s_2+p_1}\right]. \quad (18)$$

The MM has, in principle, Volterra kernels of any order. However, it can be shown that the magnitude of the nth-order kernel is proportional to the nth power of p_3, and subsequently, an adequate Volterra model may only include the first two kernels (since the value of p_3 is of the order of 10^{-5}–10^{-4}). The resulting expressions for the first- and second-order kernels in the time domain are given in (19) and (20), respectively, as shown at the bottom of this page.

These first- and second-order Volterra kernels are plotted in Fig. 2 (top panel) for typical MM parameter values within the physiological range [15], [35]: $g_b = 80\,\mathrm{mg/dL}$, $p_1 = S_G = 0.02\,\mathrm{min}^{-1}$, $p_2 = 0.028\,\mathrm{min}^{-1}$, and $p_3 = 10^{-4}\,\mathrm{min}^{-2}\cdot\mathrm{mL}/\mu\mathrm{U}$, which yield $S_I = 0.0036\,\mathrm{min}^{-1}/(\mu\mathrm{U}\cdot\mathrm{mL}^{-1})$. Since the specific parameter values define the MM description of insulin–glucose dynamics, they also define the form of the equivalent Volterra kernels. The form of the first-order kernel in Fig. 2 (top left panel) indicates that a $10\,\mu$U/mL insulin concentration increase will cause a first-order drop in plasma glucose concentration that will reach a minimum of about -1.2 mg/dL about 36 min later, rising after that to half the drop in about 1 h and relaxing back to the basal value about 4 h after the minimum. The positive values of the second-order Volterra kernel indicate that the actual glucose drop caused by the insulin infusion will be slightly less than the first-order prediction (sublinear response). For instance, an increase in insulin concentration of $100\,\mu$U/mL will not cause a maximum glucose drop of 12 mg/dL (as predicted by its equivalent first-order kernel) but a

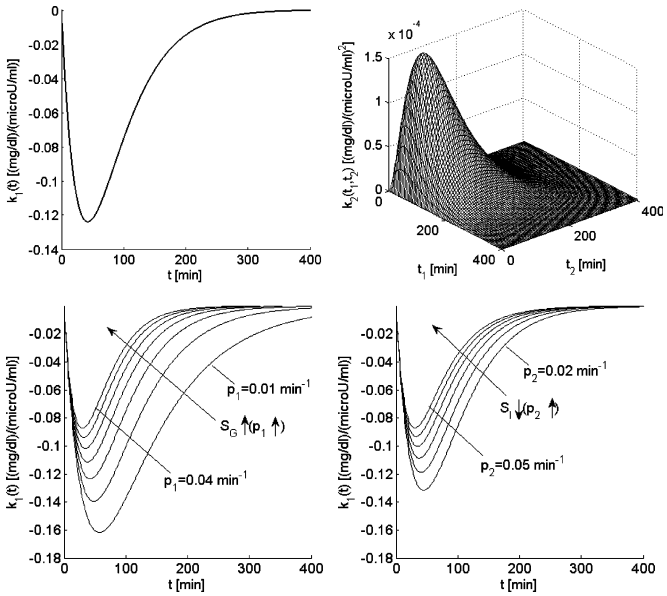

Fig. 2. (Top left) First-order and (top right) second-order Volterra kernels of the minimal model for typical values of its parameters within the physiological range ($S_G = 0.02\,\mathrm{min}^{-1}$ and $S_I = 0.0036\,\mathrm{min}^{-1}/(\mu\mathrm{U}\cdot\mathrm{mL}^{-1})$). (Bottom) Effect of the two key parameters p_1 and p_2 of the open-loop MM on the form of the equivalent first-order kernel. Note that the glucose effectiveness S_G is equal to p_1 and the insulin sensitivity S_I is inversely proportional to p_2 (and proportional to p_3). These plots offer a visual understanding of the effects of changes in these parameters (p_1 between 0.01 and $0.04\,\mathrm{min}^{-1}$, and p_2 between 0.02 and $0.05\,\mathrm{min}^{-1}$) on the first-order insulin–glucose dynamics (see text).

$$k_1(\tau) = -g_b \frac{p_3}{p_2 - p_1} \left[\exp(-p_1\tau) - \exp(-p_2\tau)\right]. \quad (19)$$

$$k_2(\tau_1, \tau_2) = \frac{g_b p_3^2}{2(p_2-p_1)^2} \left\{ \left[\exp(-p_1\tau_1) - \exp(-p_2\tau_1)\right]\left[\exp(-p_1\tau_2) - \exp(-p_2\tau_2)\right] + p_2 \left[\frac{1}{p_1} \exp[-p_1(\tau_1+\tau_2)](\exp[p_1 \min(\tau_1,\tau_2)] - 1) - \frac{1}{p_2}[\exp(-p_1\tau_1 - p_2\tau_2) + \exp(-p_1\tau_2 - p_2\tau_1)](\exp[p_2 \min(\tau_1,\tau_2)] - 1) + \frac{\exp[-p_2(\tau_1+\tau_2)]}{2p_2 - p_1}(\exp[(2p_2 - p_1)\min(\tau_1,\tau_2)] - 1) \right] \right\} \quad (20)$$

drop of about 10.5 mg/dL due to the antagonistic second-order kernel contribution.

Changes in these parameter values affect the form and the values of the kernels in the precise manner, as described by (19) and (20). The effects of changes in the two MM parameters p_1 and p_2 on the equivalent first-order kernel are illustrated in Fig. 2 (bottom panels) for a range of physiological values (p_1 between 0.01 and $0.04\,\mathrm{min}^{-1}$, and p_2 between 0.02 and $0.05\,\mathrm{min}^{-1}$ [15], keeping $p_3 = 10^{-4}\,\mathrm{min}^{-2}\cdot\mathrm{mL}/\mu\mathrm{U}$ constant). Note that changes in p_3 simply scale the first-order kernel according to (19) and do not alter its form (proportional dependence), nor do they alter the form of the second-order kernel (they scale it quadratically). A direct sense of the effects of parameter changes is obtained by the waveforms of Fig. 2, for instance, as $p_1(S_G)$ increases, the maximum drop of the first-order kernel becomes smaller and its dynamics (i.e., the drop to the minimum and the return to basal value) become faster. Similar effects are observed when p_2 increases (or S_I decreases).

B. Analytical Expressions of the Volterra Kernels of the Compartmental Model: Closed-Loop Case

To derive the analytical expressions of the kernels in the closed-loop case, we approximate the threshold function of (6) with a polynomial, as indicated next, assuming that θ is equal to zero (i.e., insulin secretion is triggered when the glucose concentration rises above its basal value)

$$\beta T_h[g(t)] \cong \beta_1 g(t) + \beta_2 g^2(t) + \cdots \tag{21}$$

where $g(t)$ is the deviation of glucose plasma concentration from its basal value. Then, (5) can be rewritten as

$$\frac{dr(t)}{dt} = -ar(t) + \beta_1 g(t) + \beta_2 g^2(t) + \cdots. \tag{22}$$

The solution of (22) is given by

$$r(t) = \beta_1 f(t) * g(t) + \beta_2 f(t) * g^2(t) + \cdots \tag{23}$$

where the asterisk denotes convolution and

$$f(t) = e^{-at}u(t). \tag{24}$$

Also, from (4), we have

$$\frac{dx(t)}{dt} = -p_3 h(t) * [i(t) + r(t)] \tag{25}$$

where

$$h(t) = e^{-p_2 t}u(t). \tag{26}$$

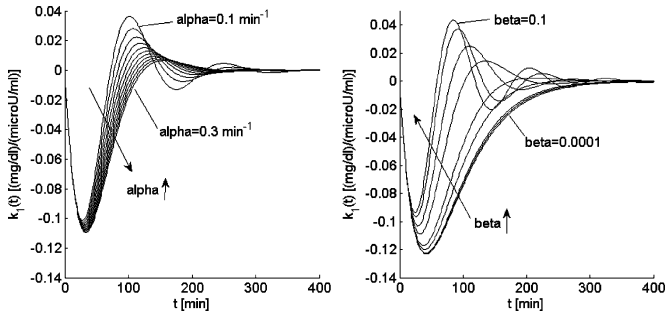

Fig. 3. First-order kernels of the AMM (left) for a, varying between 0.1 and $0.3\,\mathrm{min}^{-1}$ with constant $\beta = 0.05$, and (right) for β varying between 0.0001 and $0.1\,\mu\mathrm{U}\cdot\mathrm{min}^{-2}/(\mathrm{mL}\cdot\mathrm{mg}\cdot\mathrm{dL})$ with constant $\beta = 0.13\,\mathrm{min}^{-1}$.

Then, (3) becomes

$$\frac{dg(t)}{dt} + p_1 g(t) = -p_3 g(t)[h(t) * i(t) + \beta_1 h(t) * f(t) * g(t) + \beta_2 h(t) * f(t) * g^2(t) + \cdots]. \tag{27}$$

The aforementioned equation can be used to obtain the equivalent Volterra kernels of the closed-loop model, following the procedure outlined before for the open-loop model. The resulting expressions for the first-order and the second-order kernels in the Laplace domain are given by (28) and (29), respectively ($k_0 = 0$), (28) and (29), as shown at the bottom of this page. where $F(s)$ and $H(s)$ are the Laplace transforms of $f(t)$ and $h(t)$, respectively, i.e.

$$F(s) = \frac{1}{s+a} \tag{30}$$

$$H(s) = \frac{1}{s+p_2}. \tag{31}$$

The aforementioned relations were inverted numerically to yield the time-domain expressions for the first-order kernel, which are shown in Fig. 3 for the following parameter values: a varying between 0.1 and $0.3\,\mathrm{min}^{-1}$ with β remaining constant at $0.05\,\mu\mathrm{U}\cdot\mathrm{min}^{-2}/(\mathrm{mL}\cdot\mathrm{mg}\cdot\mathrm{dL})$ (left panel) and β varying between 0.0001 and $0.1\,\mu\mathrm{U}\cdot\mathrm{min}^{-2}/(\mathrm{mL}\cdot\mathrm{mg}\cdot\mathrm{dL})$ with a remaining constant at $0.13\,\mathrm{min}^{-1}$ (right panel). The nominal value of a ($0.13\,\mathrm{min}^{-1}$) was taken from [37], while the value of β was set at $0.05\,\mu\mathrm{U}\cdot\mathrm{min}^{-2}/(\mathrm{ml}\cdot\mathrm{mg}/\mathrm{dl})$. The decrease of a (slower insulin secretion dynamics) and increase of β (stronger feedback) similarly affect the AMM first-order kernel waveform, i.e., they result in faster dynamics with a small decrease of the

$$K_1(s) = -p_3 g_b \frac{H(s)}{s + p_1 + p_3 g_b \beta_1 H(s) F(s)} \tag{28}$$

$$K_2(s_1, s_2) = -p_3 \left\{ (\beta_2 + \beta_1) g_b \frac{H(s_1+s_2)F(s_1+s_2)K_1(s_1)K_1(s_2)}{(s_1+s_2+p_1) + p_3 g_b \beta_1 H(s_1+s_2)F(s_1+s_2)} + \frac{1}{2}\frac{H(s_1)K_1(s_2) + H(s_2)K_1(s_1)}{(s_1+s_2+p_1) + p_3 g_b \beta_1 H(s_1+s_2)F(s_1+s_2)} \right\} \tag{29}$$

negative peak value and the appearance of an overshoot, which is the characteristic of closed-loop systems.

C. Simulation Results: Open-Loop Model

In order to demonstrate the feasibility of estimating the Volterra kernels of the open-loop MM directly from input–output measurements, we simulate it by numerical integration of (1) and (2) for the following values of MM parameters: $p_1 = 0.020\,\mathrm{min}^{-1}$, $p_2 = 0.028\,\mathrm{min}^{-1}$, $p_3 = 10^{-4}\,\mathrm{min}^{-2}\cdot\mathrm{mL}/\mu\mathrm{U}$, and $g_b = 80\,\mathrm{mg/dL}$ that are around the middle of the physiological ranges reported in the literature with the exception of the value of p3, which is at the high end of this range [14], [15]. The input signal for this simulation is a zero-mean Gaussian white noise (GWN) sequence of insulin time series (i.e., independent samples every 5 min), with a standard deviation of $4\,\mu$U/mL, which may be viewed as spontaneous fluctuations around its basal value or arising from step-wise continuous infusions of insulin at random levels, changed every 5 min, superimposed on a constant (positive) baseline infusion. Due to the low-pass dynamic characteristics of the model, one sample every 5 min is sufficient for representing the input–output data. An input–output record of 144 sample points (i.e., 12-h long) is used to perform the training of the LVN and the estimation of the kernels of the equivalent Volterra model.

In order to illustrate model structure selection, we show the obtained NMSEs for various values of L, as well as for linear ($Q = 1$) and nonlinear ($Q = 2$) models for three different values of p_3, which determines the strength of the MM nonlinearity, as shown in Table I. For $p_3 = 5 \times 10^{-5}\mathrm{min}^{-2}\cdot\mathrm{mL}/\mu\mathrm{U}$, the model is weakly nonlinear, whereas for $p_3 = 5 \times 10^{-4}\,\mathrm{min}^{-2}\cdot\mathrm{mL}/\mu\mathrm{U}$, the NMSE reduction achieved for $Q = 2$ is more than 20%. The contribution of the nth-order Volterra term is proportional to the nth power of the product of parameter p_3 with the power level of the input (i.e., this contribution increases for larger insulin variations); however, for the range of values examined, a second-order model is found to be sufficient. Also, using $L > 5$ reduces the NMSE minimally in all cases. Therefore, we select a second-order LVN with one hidden unit and five Laguerre functions (i.e., $L = 5$, $K = 1$, and $Q = 2$) for the estimation of the equivalent Volterra model, with the resulting output prediction NMSE being 0.09% ($p_3 = 10^{-4}\mathrm{min}^{-2}\cdot\mathrm{mL}/\mu\mathrm{U}$). The estimated kernels of first (see Fig. 4—dotted) and second order for the noise-free case are almost identical to the true kernels given by (19) and (20) (see Fig. 2—top panel).

In order to examine the effect of measurement noise on the kernel estimates, we repeat the kernel estimation with the aforementioned input–output data after the addition of 20 independent white-noise signals with maximum amplitude equal to approximately 20% of the basal glucose value (i.e., error range of $\pm$16 mg/dL) to the output [47]. This corresponds to an SNR of around 6.5 dB relative to the demeaned glucose deviations output. The resulting kernel estimates are also shown in Fig. 4 (top panels), and they demonstrate the robustness of this modeling approach in the presence of measurement noise. The corresponding linear and nonlinear NMSEs are equal to $24.0 \pm 2.7\%$ and $23.6 \pm 2.7\%$, respectively (mean $\pm$ standard deviation), i.e., the output additive noise is not accounted by the model. Also in Fig. 4 (bottom panels), we present the kernel estimates obtained with an insulin input of the same length (144 points) composed of a random sequence of impulses (representing insulin concentration increases that could be due to insulin infusions), with a mean frequency of 1 impulse every 2 h and a normally distributed random amplitude with standard deviation $20\,\mu$U/mL. The resulting kernel estimates are almost identical to their GWN-input counterparts, demonstrating the

TABLE I
OUTPUT PREDICTION NMSEs FOR VARIOUS LVN MODEL STRUCTURES AND VALUES OF p_3, GWN INPUT (OPEN-LOOP CASE)

L	p_3=5·10^{-5} min^{-2}·$ml/\mu U$		p_3=10^{-4} min^{-2}·$ml/\mu U$		p_3=5·10^{-4} min^{-2}·$ml/\mu U$	
	Linear NMSE	Nonlinear NMSE	Linear NMSE	Nonlinear NMSE	Linear NMSE	Nonlinear NMSE
2	13.55	8.97	16.24	15.46	22.42	4.89
3	0.39	0.32	0.68	0.30	23.23	1.13
4	4.62	4.85	3.33	3.63	23.88	3.73
5	0.17	0.14	0.40	0.09	21.35	0.61
6	0.22	0.31	0.39	0.17	21.82	0.61
7	0.10	0.04	0.36	0.05	21.49	0.61

The value of p_3 determines the relative contribution of the nonlinear terms: note that for $p_3 = 5 \times 10^{-5}$ $\mathrm{min}^{-2}\cdot\mathrm{mL}/\mu\mathrm{U}$, the NMSE reduction achieved by nonlinear models is marginal, while for 5×10^{-4} $\mathrm{min}^{-2}\cdot\mathrm{mL}/\mu\mathrm{U}$, it is more than 20%. Using $L > 5$ does not improve model performance further.

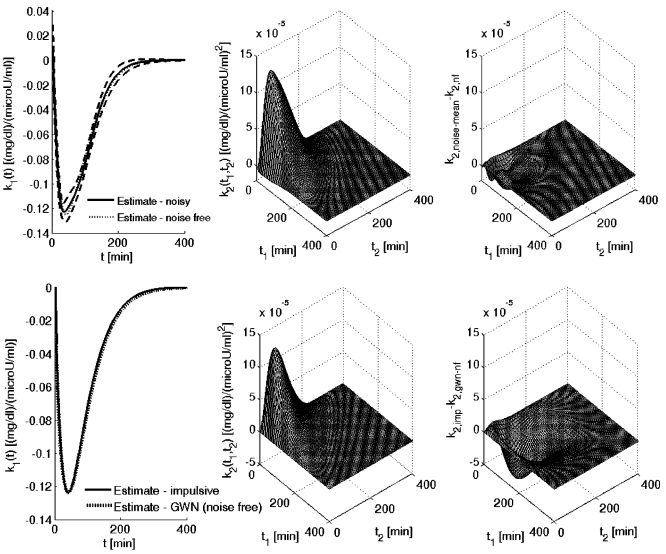

Fig. 4. (Top) Estimated first- and second-order Volterra kernels of the MM using a GWN input of 144 points (12 h) when 20 different realizations of independent GWN signals are added to the output for an SNR of 6.5 dB. The obtained first-order (left—solid line: mean value; dashed line: $\pm$ one standard deviation; and dotted line: noise-free estimate) and second-order kernel estimates (middle—mean value) are not affected significantly relative to their exact counterparts (Fig. 2—top), demonstrating the robustness of this approach. (Bottom) Estimated first- and second-order Volterra kernels of the MM for an insulin input composed of eight insulin infusions over 12 h. The timing and amplitude of each infusion are random (see text). Note the similarity of these estimates to the estimates obtained from GWN inputs. (Right): Difference between averaged noisy output (top), impulse input (bottom) and noise-free second-order kernel estimates.

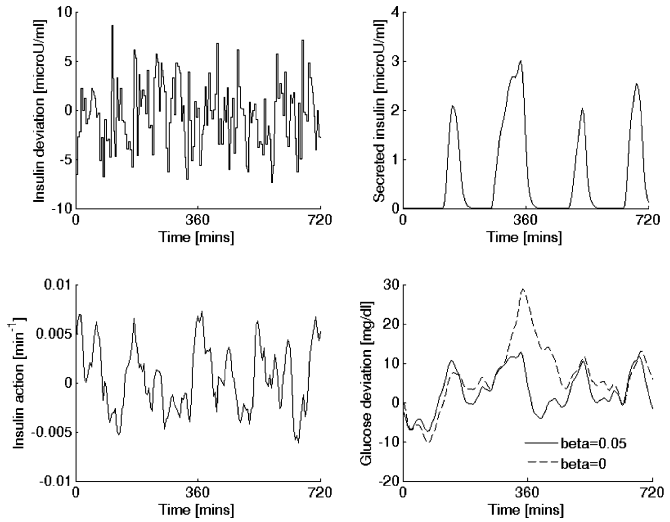

Fig. 5. Representative realization of the closed-loop AMM time-series data for a GWN insulin input used for LVN training (length: 12 h). The insulin time series represent deviations from its basal value. The effect of the secretion equation is seen by comparing the two output waveforms of glucose deviations shown in the bottom right panel (dashed line: open loop and solid line: closed loop for $\beta = 0.05$).

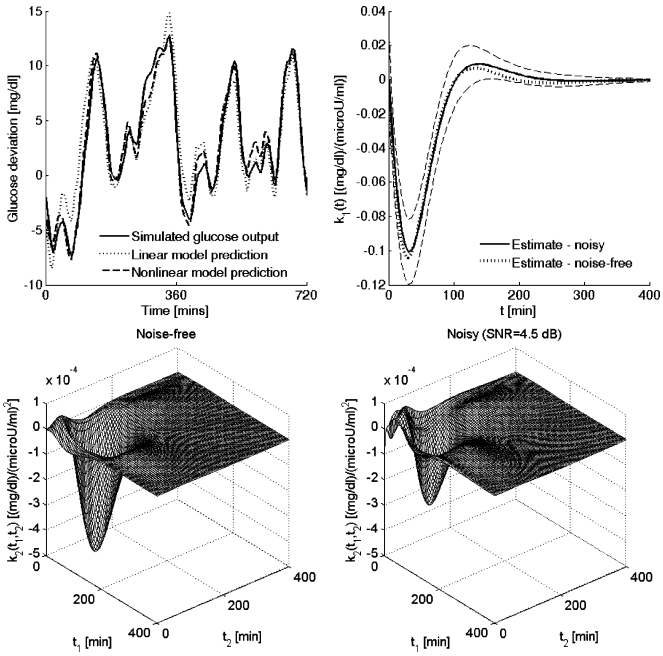

Fig. 6. Representative model predictions (top left) and estimated first and second order Volterra kernels of the closed-loop AMM for a GWN input of 144 points (12 hrs) for noise-free output (top right—dotted and bottom left respectively) and when 20 different realizations of independent GWN measurement noise are added to the output for an SNR of 4.5 dB (top right—solid black: mean, dashed black: $\pm$ one standard deviation and bottom right—mean).

feasibility of estimating accurate Volterra models using sparser, infusion-like stimuli.

D. Simulation Results: Closed-Loop Model

The closed-loop AMM was simulated with the same GWN input used for the open-loop MM by numerical integration of (3)–(5), for $p_1 = 0.020\,\mathrm{min}^{-1}, p_2 = 0.028\,\mathrm{min}^{-1}$, and $p_3 = 10^{-4}\,\mathrm{min}^{-2}\cdot\mathrm{mL}/\mu\mathrm{U}$, and parameter values of $a = 0.13\,\mathrm{min}^{-1}, \beta = 0.05\,\mu\mathrm{U}\cdot\mathrm{min}^{-2}/(\mathrm{mL}\cdot\mathrm{mg}\cdot\mathrm{dL})$, and $\theta = 80$ mg/dL for the additional insulin-secretion equation. Representative time-series data of the resulting insulin input, insulin secretion, insulin action, and glucose, used for training the equivalent LVN model, are shown in Fig. 5, where the effect of insulin secretion, relative to the open-loop case, can be seen in the bottom right panel (solid line: closed-loop output and dashed line: open-loop output).

An LVN with $L = 5$, $K = 2$, and $Q = 3$ was employed in this case, i.e., a more complex structure of higher order is required relative to the open-loop case. In the noise-free case, the obtained nonlinear model reduces the prediction NMSE considerably, from 12.41%—yielded by the linear model—to 2.18% (see Fig. 6, top left panel). As before, we repeat the kernel estimation after adding 20 independent white noise sample signals (with the same variance as before) to the output. Note that the resulting SNR is now around 4.5 dB, i.e., lower than the open-loop case, since the noise-free output (glucose deviations) has a smaller mean-square value in the closed-loop case, due to the effect of the endogenous insulin secretion. Therefore, the corresponding NMSEs are larger, i.e., 48.2% for the linear model and $34.2 \pm 4.0\%$ for the nonlinear model, and correspond, for the nonlinear model, to the noise content. This demonstrates the predictive capability of the obtained models in the presence of considerable output-additive noise that emulates the observed errors in the measurements of current continuous glucose monitors [47]. The kernel estimates for both cases are shown in Fig. 6, illustrating the robustness of this approach. The first- and second-order kernels of the closed-loop AMM exhibit biphasic characteristics (i.e., regions of positive and negative response to a positive change in the input, and *vice versa*). The first-order kernel contribution to the output remains dominant over the second-order kernel contribution for impulsive inputs up to about $100\,\mu$U/mL.

The obtained equivalent PDM models for both the open-loop and closed-loop models are shown in Fig. 7. In the open-loop case (top panel), since we have used $K = 1$ in the LVN model, the equivalent PDM model has one branch with the PDM dynamics exhibiting similar characteristics to the open-loop first-order kernel (see Fig. 2) and the static nonlinearity being close to linear. In the closed-loop case (bottom panel), we have used $K = 2$, and therefore, the equivalent PDM model has two branches. The lower PDM exhibits a clear biphasic response characteristic (corresponding to a glucose decrease and increase, respectively, in response to an insulin increase) that is not present in the open-loop model. The upper PDM branch exhibits slower dynamics (peak latency of about 80 min) than the open-loop PDM (peak latency at 40 min) and a strictly negative nonlinearity (i.e., always leading to a reduction of glucose), while the nonlinearity of the open-loop model has both positive and negative response regions. The PDM of the lower branch exhibits faster dynamics (shorter latency of the first peak of about 30 min), and has a nonlinearity that resembles a sigmoidal (soft saturating) characteristic.

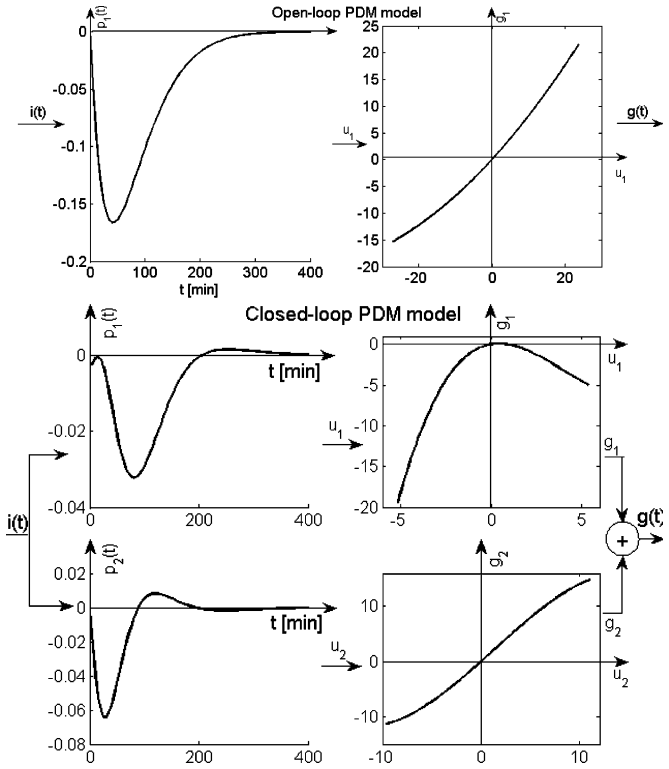

Fig. 7. (Top and bottom) Obtained PDM model for the open- and closed-loop models, which consist of one and two branches, respectively. (Top left) The open-loop single PDM exhibits a glucoleptic characteristic (reduces the glucose output) for positive insulin inputs in a mildly sublinear manner. The closed-loop upper PDM branch exhibits a glucoleptic characteristic for positive or negative insulin inputs in a mildly supralinear manner, unlike the single PDM branch of the open-loop MM. Note that the latency of the peak response (about 80 min) is much longer for this closed-loop PDM than for the open-loop PDM (about 40 min), and the slope of its output nonlinearity is different for positive/negative input (about 4 to 1). The lower PDM is biphasic with the first glucoleptic peak having a latency comparable to the open-loop PDM (about 30 min), and the second glucogenic peak being much smaller (about 15%) and having a latency of about 120 min. The nonlinearity of the lower PDM branch retains the biphasic response characteristic (increase of insulin leads to glucose decrease and *vice versa*), and is mildly sublinear (resembling a soft saturating characteristic).

IV. Discussion

In the present paper, we have rigorously examined the relation between nonlinear compartmental and Volterra models of glucose metabolism. Two widely used compartmental models, the MM of glucose disappearance and its closed-loop extension (AMM), which includes the effects of insulin secretion, were formulated in the Volterra–Wiener framework and equivalent descriptions, in the form of Volterra models, were derived analytically. The effect of parametric compartmental model parameters of clinical importance on these descriptors (Volterra kernels) was examined. Using the simulated data generated from the aforementioned compartmental models, we have demonstrated the feasibility of obtaining Volterra models that describe these data accurately, using both random-like and impulsive insulin stimuli. We have also shown that these estimates are not affected significantly by output-additive noise corresponding to measurement noise. The results provide evidence that Volterra models, free of *a priori* assumptions, may be estimated reliably from patient-specific data. These models may provide quantitative descriptions that reflect the underlying physiological mechanisms under general operating conditions, and may prove useful in diagnostic or therapeutic (e.g., for glucose regulation—for an initial report, see [48]) applications. This should be further verified using glucose disturbance patterns and experimental data from diabetic patients, a task that is currently underway. We should note that for model-based glucose control applications, additional factors, such as the delay between plasma glucose and the sensor signal, should be taken into account.

The parametric models examined herein are nonlinear due to the presence of a bilinear term in (1) and (3), which modulates the effective time constant of glucose disappearance and depends on the action of plasma insulin (in the case of MM), and both plasma and endogenous secreted insulin (in the case of AMM), respectively. An additional nonlinearity is found in the endogenous insulin-secretion equation (5) of the AMM in the form of a nonlinear threshold operator. The range of values for the MM and AMM parameters is taken from the literature [14], [15], [34]–[37]. The value of p_3 was selected toward the upper limit of previously reported values in order to increase the contribution of the bilinear term. Note that in the more general case, the value of β could be viewed as being dependent on g, in order to account for the effect of blood glucose concentration on insulin secretion. The value of the threshold θ in the endogenous insulin-secretion equation (5) was selected to be equal to zero in order to simplify the analytical derivations. This threshold can be generally set to a larger value, particularly, when glucose disturbance terms that are noninsulin-dependent, are included. However, in the context of the simulations presented herein, this value yielded reasonable patterns for the insulin secretion profile (see Fig. 5).

Two types of inputs (variations of insulin concentration) were used in this computational study for the simulation of the parametric models: GWN fluctuations around a putative basal value (corresponding to the GWN mean) and random sequences of sparse insulin increases (about one every 2 h on the average), which may result from insulin/glucose infusions. It was shown that reliable and robust nonparametric models can be obtained with both types of stimuli in the presence of measurement noise. The GWN insulin fluctuations may also be viewed as internal spontaneous fluctuations, and therefore, the applicability of this approach can be extended to the case of spontaneous glucose/insulin measurements. The use of random sequences of larger sparse impulsive insulin increases, although unconventional, was shown to be effective in terms of model estimation, and may offer clinical advantages as it is likely to mitigate the risk of induced hypoglycemia—an issue that must be examined carefully in future studies.

The Volterra approach does not require specific prior postulates of compartmental model structures (e.g., it is not committed to any particular number of compartments), and allows estimation of the model (i.e., the Volterra kernels) directly from arbitrary input–output data. Therefore, it offers the advantage of yielding models that are "true-to-the-data" and valid under all input conditions within the range of the experimental data. Therefore, this fundamentally different approach provides

significant benefits relative to existing approaches in terms of modeling flexibility and accuracy.

The robustness of the Volterra modeling approach (i.e., the effect of output-additive noise on the obtained kernel estimates) was studied the selecting as noise sample signals from a GWN process with variance consistent with what is known about glucose measurement errors (i.e., a standard deviation equal to 14%–20% of the glucose basal value [47]). However, we must make the distinction between *noise* (which is primarily related to measurement errors) and systemic *disturbance* (which is related to systemic perturbations that are not explicitly accounted for in the model). The systemic disturbance signal may include the effect of meals [49], the effect of circadian and ultradian endocrine cycles [50], and the effect of randomly occurring events of accelerated metabolism (due to exercise or physical exertion) as well as neurohormonal excretions (due to stress or mental exertion). The amplitudes and the relative phases of these disturbance components will generally vary among subjects and over time. Since the selection of such disturbance components is rather complex, the study of their effect on the robustness of the model estimation is deferred to future studies.

The MM approach is based on the notion that estimates of the three model parameters (p_1, p_2, and p_3), obtained through a glucose tolerance test, provide the necessary clinical information for diagnostic purposes in the form of the equivalent indexes of glucose effectiveness (S_G) and insulin sensitivity (S_I). Although this proposition has merit and has proven to be useful so far, it is widely recognized that it has serious limitations [15], [19], [20]. To overcome some of these potential limitations, our approach advances the notion that a Volterra-type model (in the form of kernels or the PDM model) provides the requisite clinical information in a more complete manner (i.e., no model constraints). In order to compare the relative utility of the Volterra approach with the conventional MM approach in a clinical context, we must define clinically relevant attributes for the two approaches that are directly comparable. For instance, if we are interested in deriving quantitative descriptions/measures of how insulin affects the plasma glucose concentration in specific subjects (i.e., based on collected data), we may use certain features of the estimated first-order kernels, such as the integrated area, peak value, and initial slope, which determine the linear component of the overall effect of an insulin injection, its maximum instantaneous effect, and how fast this effect occurs, respectively, instead of the estimated MM parameters.

In this context, the combined effect of errors in the estimates of the three parameters of the MM (p_1, p_2, and p_3) may be compared to estimation errors in the integrated area of the first-order kernel, which is equal to the ratio S_I/S_G (i.e., $p_3/(p_1 p_2)$), as a measure of how much a unitary insulin impulse will affect the plasma glucose concentration. Also, since $S_G = p_1$ is the inverse of the long time-constant of the kernel (providing a measure of the extent of the kernel), it follows that "insulin sensitivity" S_I is akin to the average kernel value. Thus, one may suggest that the clinical index of "insulin sensitivity" may be defined alternatively by the average kernel value and "glucose effectiveness" by the extent of the kernel in the data-driven modeling context. It also stands to reason that the peak value of this kernel is likely to have some clinical significance, since it quantifies the maximum effect of an insulin injection on blood glucose in a given subject. Finally, the slope of the first-order kernel at the origin (a measure of how rapidly glucose drops in response to an insulin infusion) is equal to—($g_b p_3$). Since the basal glucose value is known, a quick estimate of p_3 can be obtained from the slope of the first-order kernel. In the aforementioned context, PDM models (see Fig. 7) may prove very beneficial, since they facilitate meaningful physiological interpretations relative to the general Volterra formulation. Therefore, certain characteristics of the PDM branches (e.g., the dynamics of the linear filters and the characteristics of the nonlinearities) may also be associated to clinical indexes that describe insulin action and its efficiency in specific subjects.

TABLE II
MEAN AND SD OF ESTIMATED FEATURES OF THE FIRST-ORDER KERNEL FOR THE SIMULATED MM DATA OVER 20 RUNS IN THE CASE OF NOISY OUTPUT AT SNR + 6.5 dB

First-order kernel features	Noise-free	Noisy (SNR=6.5 dB) (Mean ± SD)
Area	13.95	13.94 ± 1.03
Peak value	-0.124	-0.125 ± 0.007
Time to peak	45	42.3 ± 6.8
Initial slope	-0.0079	-0.0078 ± 0.0018

The rms of the noise-free output is approximately twice the noise SD. The values of these kernel features have specific analytical relations with the MM parameters p_1, p_2, and p_3 (see text). For example, the values of p_3 that correspond to the estimated initial slope are 9.88×10^{-5} min^{-2} mL/μU (noise-free case) and $(9.68 \pm 2.23) \times 10^{-5}$ min^{-2}·mL/μU (noisy output), respectively.

As a first illustration, we provide the estimates of several first-order kernel features in the presence of noise in Table II, in the case of the open-loop MM (see Fig. 4—top panel). It can be seen that the effect of output additive noise is smaller in the estimated kernel feature values (variation coefficient between 8% and 25%) than in the output data (variation coefficient of 50%). However, the relative utility of these different measures in a clinical context will also depend on the robustness of their estimation in the presence of systemic disturbances; therefore, it is an issue that deserves further attention and must be examined in future studies.

Finally, we present results from fitting the MM and LVN models to simulated data obtained from the model proposed by Sorensen [25], which has been used as a comprehensive representation of the metabolic system in several studies (e.g., [29] and [35]) for insulin input signals considered before (i.e., random insulin variations around a putative basal value). Note that we do not make claims about the universal validity of this particular model, but we use it as a third-party metabolic simulator for comparative purposes. We considered two distinct cases of Sorensen model parameters: one that corresponds to a healthy subject and another that corresponds to a type-1 diabetic subject, following the procedure described in [39]. The MM parameters were obtained by using a nonlinear optimization method (Levenberg–Marquardt method) in order to fit p_1, p_2, and p_3 to the Sorensen-model-generated data. We considered ten different realizations of the insulin input signal (of the same length as considered before) and provide the results in Table III and Fig. 8. The results show that the output prediction performance of the LVN model is superior in both cases, particularly for the

TABLE III
COMPARATIVE RESULTS OBTAINED FROM FITTING MM AND LVN MODELS TO SIMULATED DATA OBTAINED FROM THE SORENSEN MODEL FOR TEN DIFFERENT RANDOM INSULIN INPUTS (VARIATIONS AROUND A PUTATIVE BASAL VALUE)

	Healthy	Type-1 diabetic
LVN NMSE [%]	3.62±1.92	4.95±4.90
MM NMSE [%]	11.11±7.52	25.37±10.73
p_1 [min^{-1}]	0.016±0.006	0.028±0.015
p_2 [min^{-1}]	0.058±0.024	0.042±0.009
p_3 [$min^{-2}\cdot ml/\mu U$]	$(1.31\pm0.24)\cdot10^{-5}$	$(1.52\pm0.53)\cdot10^{-5}$

The obtained NMSE values correspond to the demeaned glucose output data. The LVN models yielded better prediction performance overall, particularly in the type-1 diabetic case, while the obtained MM parameter estimates were influenced considerably by the particular input realization. Values are Mean ± SD.

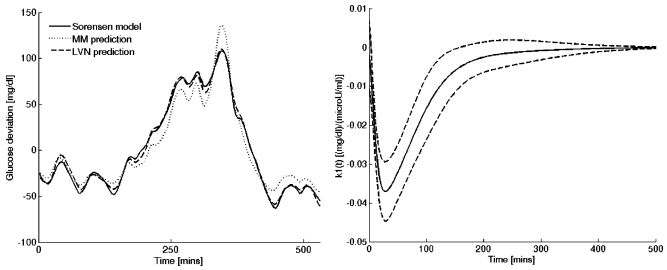

Fig. 8. (Left) Predictions of the MM and LVN models for a representative Sorensen-model-simulated dataset (healthy subject). (Right) Average first-order kernel estimate of the LVN model for ten different insulin input realizations. Solid black line: mean; dashed line: ± one standard deviation.

type-1 diabetic case. We note that an LVN model structure with $L = 5, K = 1$, and $Q = 2$ was deemed appropriate in this case.

The presented results demonstrate the relative advantages and disadvantages of the Volterra modeling methodology versus the compartmental approach for these particular parametric models (MM and AMM). The Volterra approach is inductive (data-driven), and yields models with minimum prior assumptions [38]. The compartmental approach is deductive (hypothesis-based), and yields models with the desired level of complexity that are directly interpretable but not necessarily inclusive of all functional characteristics of the system. The recent availability of continuous measurements of glucose (through continuous glucose sensors) and the feasibility of frequent infusions of insulin (through implantable insulin micropumps) make possible for the first time the realistic application of data-driven modeling approaches in a subject-specific and adaptive context, which does not require the prior postulates of compartmental models. The potential benefits include the inherent completeness of the obtained models (in the sense that they will include all functional characteristics of the system contained within the data), the robustness of its estimation in a practical context, its subject-specific customization, and its time-dependent adaptability when the system characteristics are changing slowly over time allowing effective tracking of these changes in each specific subject.

REFERENCES

[1] The Diabetes Control and Complications Trial Research, "The effect of intensive treatment of diabetes on the development and progression of long-term complications in insulin-dependent diabetes mellitus," *New England J. Med.*, vol. 329, pp. 977–986, 1993.

[2] A. D. Association, "Standards of medical care in diabetes—2008," *Diabetes Care*, vol. 31, pp. S12–S54, 2008.

[3] J. Radziuk and S. Pye, "Hepatic glucose uptake, gluconeogenesis and the regulation of glycogen synthesis," *Diabetes/Metab. Res. Rev.*, vol. 17, pp. 250–272, 2001.

[4] J. D. McGarry and R. L. Dobbins, "Fatty acids, lipotoxicity and insulin secretion," *Diabetologia*, vol. 42, pp. 128–138, 1999.

[5] N. Porksen, "The in vivo regulation of pulsatile insulin secretion," *Diabetologia*, vol. 45, pp. 3–20, 2002.

[6] P. D. Feo, G. Perriello, E. Torlone, M. M. Ventura, C. Fanelli, F. Santeusanio, P. Brunetti, J. E. Gerich, and G. B. Bolli, "Contribution of cortisol to glucose counter regulation in humans," *AJP—Endocrinol. Metab.*, vol. 257, pp. E35–E42, 1989.

[7] N. Eigler, L. Saccà, and R. S. Sherwin, "Synergistic interactions of physiologic increments of glucagon, epinephrine, and cortisol in the dog," *J. Clin. Invest.*, vol. 63, pp. 114–123, 1979.

[8] D. E. James, K. M. Burleigh, and E. W. Kraegen, "In vivo glucose metabolism in individual tissues of the rat. Interaction between epinephrine and insulin," *J. Biol. Chem.*, vol. 261, pp. 6366–6374, 1986.

[9] V. W. Bolie, "Coefficients of normal blood glucose regulation," *J. Appl. Physiol.*, vol. 16, pp. 783–788, Sep. 1961.

[10] E. Ackerman, L. C. Gatewood, J. W. Rosevear, and G. D. Molnar, "Model studies of blood-glucose regulation," *Bull. Math. Biophys.*, vol. 27, pp. 21–37, 1965.

[11] E. R. Carson, C. Cobelli, and L. Finkelstein, *The Mathematical Modeling of Endocrine-Metabolic Systems. Model Formulation, Identification and Validation*. New York: Wiley, 1983.

[12] R. N. Bergman, Y. Z. Ider, C. R. Bowden, and C. Cobelli, "Quantitative estimation of insulin sensitivity," *Amer. J. Physiol.*, vol. 236, pp. E667–E677, Jun. 1979.

[13] R. N. Bergman and J. C. Lovejoy, *The Minimal Model Approach and Determinants of Glucose Tolerance,* vol. 7. Baton Rouge, LA: Louisiana State Univ. Press, 1997.

[14] R. N. Bergman, S. M. Phillips, and C. Cobelli, "Physiologic evaluation of factors controlling glucose tolerance in man: Measurement of insulin sensitivity and beta-cell glucose sensitivity from the response to intravenous glucose," *J. Clin. Invest.*, vol. 68, pp. 1456–1467, 1981.

[15] T. C. Ni, M. Ader, and R. N. Bergman, "Reassessment of glucose effectiveness and insulin sensitivity from minimal model analysis: A theoretical evaluation of the single-compartment glucose distribution assumption," *Diabetes*, vol. 46, pp. 1813–21, Nov. 1997.

[16] K. E. Andersen and M. Hojbjerre, "A population-based Bayesian approach to the minimal model of glucose and insulin homeostasis," *Statist. Med.*, vol. 24, pp. 2381–2400, Aug. 15, 2005.

[17] I. F. Godsland, O. F. Agbaje, and R. Hovorka, "Evaluation of nonlinear regression approaches to estimation of insulin sensitivity by the minimal model with reference to Bayesian hierarchical analysis," *Amer. J. Physiol. Endocrinol. Metab.*, vol. 291, pp. E167–E174, Jul. 2006.

[18] K. M. Krudys, S. E. Kahn, and P. Vicini, "Population approaches to estimate minimal model indexes of insulin sensitivity and glucose effectiveness using full and reduced sampling schedules," *Amer. J. Physiol. Endocrinol. Metab.*, vol. 291, pp. E716–E723, Oct. 2006.

[19] A. Caumo, P. Vicini, and C. Cobelli, "Is the minimal model too minimal?" *Diabetologia*, vol. 39, pp. 997–1000, Aug. 1996.

[20] C. Cobelli, F. Bettini, A. Caumo, and M. J. Quon, "Overestimation of minimal model glucose effectiveness in presence of insulin response is due to undermodeling," *Amer. J. Physiol.*, vol. 275, pp. E1031–E1036, Dec. 1998.

[21] T. Callegari, A. Caumo, and C. Cobelli, "Bayesian two-compartment and classic single-compartment minimal models: Comparison on insulin modified IVGTT and effect of experiment reduction," *IEEE Trans. Biomed. Eng.*, vol. 50, no. 12, pp. 1301–1309, Dec. 2003.

[22] A. Caumo, P. Vicini, J. J. Zachwieja, A. Avogaro, K. Yarasheski, D. M. Bier, and C. Cobelli, "Undermodeling affects minimal model indexes: Insights from a two-compartment model," *Amer. J. Physiol.*, vol. 276, pp. E1171–E1193, Jun. 1999.

[23] P. Vicini, A. Caumo, and C. Cobelli, "The hot IVGTT two-compartment minimal model: Indexes of glucose effectiveness and insulin sensitivity," *Amer. J. Physiol. Endocrinol. Metab.*, vol. 273, pp. E1024–E1032, Nov. 1997.

[24] C. Cobelli and A. Mari, "Validation of mathematical models of complex endocrine-metabolic systems. A case study on a model of glucose regulation," *Med. Biol. Eng. Comput.*, vol. 21, pp. 390–399, Jul. 1983.

[25] J. Sorensen "A physiologic model of glucose metabolism in man and its use to design and assess improved insulin therapies for diabetes," Ph.D.

dissertation, Dept. Chem. Eng., Massachusetts Inst. Technol., Cambridge, MA, 1985.
[26] V. Tresp, T. Briegel, and J. Moody, "Neural-network models for the blood glucose metabolism of a diabetic," *IEEE Trans. Neural Netw.*, vol. 10, no. 5, pp. 1204–1213, Sep. 1999.
[27] S. Andreassen, J. J. Benn, R. Hovorka, K. G. Olesen, and E. R. Carson, "A probabilistic approach to glucose prediction and insulin dose adjustment: Description of metabolic model and pilot evaluation study," *Comput. Methods Prog. Biomed.*, vol. 41, pp. 153–165, Jan. 1994.
[28] J. A. Florian and R. S. Parker, "Empirical modeling for glucose control in diabetes and critical care," *Eur. J. Control*, vol. 11, pp. 605–616, 2005.
[29] R. S. Parker, F. J. Doyle, 3rd, and N. A. Peppas, "A model-based algorithm for blood glucose control in type I diabetic patients," *IEEE Trans. Biomed. Eng.*, vol. 46, no. 2, pp. 148–157, Feb. 1999.
[30] A. Roy and R. S. Parker, "Dynamic modeling of free fatty acid, glucose, and insulin: An extended "minimal model"," *Diabetes Technol. Ther.*, vol. 8, pp. 617–626, Dec. 2006.
[31] B. W. Bode, H. T. Sabbah, T. M. Gross, L. P. Fredrickson, and P. C. Davidson, "Diabetes management in the new millennium using insulin pump therapy," *Diabetes Metab. Res. Rev.*, vol. 18, pp. S14–S20, Jan./Feb. 2002.
[32] G. Freckmann, B. Kalatz, B. Pfeiffer, U. Hoss, and C. Haug, "Recent advances in continuous glucose monitoring," *Exp. Clin. Endocrinol. Diabetes*, vol. 109, pp. S347–S357, 2001.
[33] T. Bremer and D. A. Gough, "Is blood glucose predictable from previous values? A solicitation for data," *Diabetes*, vol. 48, pp. 445–451, 1999.
[34] S. M. Furler, E. W. Kraegen, R. H. Smallwood, and D. J. Chisolm, "Blood glucose control by intermittent loop closure in the basal model: Computer simulation studies with a diabetic model," *Diabetes Care*, vol. 8, pp. 553–561, 1985.
[35] S. M. Lynch and B. W. Bequette, "Model predictive control of blood glucose in Type 1 diabetics using subcutaneous glucose measurements," in *Proc. Amer. Control Conf.*, Anchorage, AK, 2002, pp. 4039–4043.
[36] G. Toffolo, R. N. Bergman, D. T. Finegood, C. R. Bowden, and C. Cobelli, "Quantitative estimation of beta cell sensitivity to glucose in the intact organism: A minimal model of insulin kinetics in the dog," *Diabetes*, vol. 29, pp. 979–990, Dec. 1980.
[37] T. V. Herpe, B. Pluymers, M. Espinoza, G. V. den Berghe, and B. D. Moor, "A minimal model for glycemia control in critically ill patients," in *Proc. 28th IEEE EMBS Annu. Int. Conf.*, New York, 2006, pp. 5432–5435.
[38] V. Z. Marmarelis, *Nonlinear Dynamic Modeling of Physiological Systems*. Piscataway, NJ: IEEE–Wiley, 2004.
[39] M. G. Markakis, G. D. Mitsis, and V. Z. Marmarelis, "Computational study of an augmented minimal model for glycemia control," in *Proc. 30th Annu. IEEE-EMBS Conf*, Vancouver, BC, Canada, 2008, pp. 5445–5448.
[40] G. M. Steil, K. Rebrin, R. Janowski, C. Darwin, and M. F. Saad, "Modeling beta-cell insulin secretion—Implications for closed-loop glucose homeostasis," *Diabetes Technol. Ther.*, vol. 5, pp. 953–964, 2003.
[41] G. Toffolo, M. Campioni, R. Basu, R. A. Rizza, and C. Cobelli, "A minimal model of insulin secretion and kinetics to assess hepatic insulin extraction," *Amer. J. Physiol. Endocrinol. Metab.*, vol. 290, pp. E169–E176, Jan. 2006.
[42] G. D. Mitsis and V. Z. Marmarelis, "Modeling of nonlinear physiological systems with fast and slow dynamics. I. Methodology," *Ann. Biomed. Eng.*, vol. 30, pp. 272–281, Feb. 2002.
[43] V. Z. Marmarelis and X. Zhao, "Volterra models and three-layer perceptrons," *IEEE Trans. Neural Netw.*, vol. 8, pp. 1421–1433, 1997.
[44] J. Sjoberg, *Non-linear System Identification With Neural Networks*. Linkoping, Sweden: Linkoping Univ., 1995.
[45] V. Z. Marmarelis, "Modeling methodology for nonlinear physiological systems," *Ann. Biomed. Eng.*, vol. 25, pp. 239–251, 1997.
[46] V. Z. Marmarelis, "Wiener analysis of nonlinear feedback in sensory systems," *Ann. Biomed. Eng.*, vol. 19, pp. 345–382, 1991.
[47] J. Ginsberg, "The current environment of CGM technologies," *J. Diabetes Sci. Technol.*, vol. 1, pp. 111–127, 2007.
[48] M. G. Markakis, G. D. Mitsis, G. P. Papavassilopoulos, and V. Z. Marmarelis, "Model predictive control of blood glucose in type 1 diabetics: The principal dynamic modes approach," in *Proc. 30th Annu. IEEE-EMBS Conf.*, Vancouver, BC, Canada, 2008, pp. 5466–5469.
[49] M. E. Fisher, "A semiclosed-loop algorithm for the control of blood glucose levels in diabetics," *IEEE Trans. Biomed. Eng.*, vol. 38, no. 1, pp. 57–61, Jan. 1991.
[50] E. V. V. Cauter, E. T. Shapiro, H. Tillil, and K. S. Polonsky, "Circadian modulation of glucose and insulin responses to meals—Relationship to cortisol rhythm," *Amer. J. Physiol.*, vol. 262, pp. R467–R475, 1992.

Georgios D. Mitsis (S'99–M'02) was born in Ioannina, Greece, in 1975. He received the Diploma in electrical and computer engineering from the National Technical University of Athens, Athens, Greece, in 1997, two M.S. degrees in biomedical and electrical engineering, and the Ph.D. degree in biomedical engineering from the University of Southern California, Los Angeles, in 2000, 2001, and 2002, respectively.

He was a Postdoctoral Researcher at Biomedical Simulations Resource, Los Angeles, CA, and Oxford Centre for Functional Magnetic Resonance Imaging (FMRIB), University of Oxford, U.K. He was an ENTER Research Fellow with the National Technical University of Athens. He joined the Department of Electrical and Computer Engineering, University of Cyprus, Nicosia, Cyprus, where he is currently a Lecturer. His current research interests include nonlinear and nonstationary systems identification, with applications to quantitative/systems biology and physiology, as well as functional magnetic resonance imaging of the brain.

Dr. Mitsis is a member of the Technical Chamber of Greece. He is currently an Associate Editor for the Annual IEEE Engineering in Medicine and Biology Society (EMBS) Conference (Biosignal Processing Theme).

Mihalis G. Markakis (S'07) was born in Athens, Greece, in 1982. He received the B.S. degree from the National Technical University of Athens, Athens, in 2005, and the M.S. degree from the University of Southern California, Los Angeles, in 2008, both in electrical engineering. He is currently working toward the Ph.D. degree at the Laboratory for Information and Decision Systems, Massachusetts Institute of Technology, Cambridge.

His current research interests include modeling and control of dynamic and stochastic systems, with applications ranging from physiological systems to communication networks.

Vasilis Z. Marmarelis (M'79–SM'94–F'97) was born in Mytilini, Greece, on November 16, 1949. He received the Diploma in electrical and mechanical engineering from the National Technical University of Athens, Athens, Greece, in 1972, and the M.S. and Ph.D. degrees in engineering science (information science and bioinformation systems) from the California Institute of Technology, Pasadena, in 1973 and 1976, respectively.

For two years, he was a Postdoctoral Researcher at the California Institute of Technology. He then joined the faculty of Biomedical and Electrical Engineering, University of Southern California, Los Angeles, where he is currently a Professor and the Director of the Biomedical Simulations Resource. From 1990 to 1996, he was the Chairman of the Biomedical Engineering Department, University of Southern California, Los Angeles, CA. He has coauthored the books *Analysis of Physiological Systems: The White-Noise Approach* (New York: Plenum, 1978; Russian translation: Moscow, Russia: Mir Press, 1981; Chinese translation: Beijing, China: Acad. Sci. Press, 1990) and *Nonlinear Dynamic Modeling of Physiological Systems* (Piscataway, NJ: Wiley/IEEE, 2004). He was the Editor of three volumes of *Advanced Methods of Physiological System Modeling* (1987, 1989, and 1994). He has authored or coauthored more than 100 papers and book chapters in the area of system and signal analysis. His current research interests include nonlinear and nonstationary system identification and modeling, with applications to biology, medicine, and engineering systems, spatiotemporal and nonlinear/nonstationary signal processing, and analysis of neural systems and networks with regard to information processing.